Wannes et al., J Textile Sci Eng 2018, 8:1
DOI: 10.4172/2165-8064.1000329

Journal of Textile Science & Engineering

Research Article Open Access

Effect of Experimental Condition on Properties of Zinc Oxide Films Prepared by Sol-Gel Deposition with Ammonium Hydroxide as an Additive

Wannes BH[1,2]*, Zaghouania BR[1] and Dimassia W[1]

[1]*Photovoltaic Laboratory, Research and Technologies Centre of Energy, Technopark of Borj Cedria, Tunisia*
[2]*Faculty of Sciences of Tunis, University Tunis El Manar, Tunisia*

Abstract

In this work, we report on the study of undoped zinc oxide (ZnO) thin films prepared by sol-gel spin coating technique using the ammonium hydroxide as an additive. The effect of the precursor concentration and the annealing temperature on the optical and structural properties of the produced films is analyzed; we changed the precursor concentration and the annealing temperature from 0.1 M to 0.2 M and 400°C to 500°C with steps of 0.1M and 100°C, respectively. X-ray diffraction (XRD) results show that ZnO thin films are polycrystalline with a hexagonal structure and preferred growth orientations along the a-axis (100) and c-axis (002) from the substrate surface. The elaborated films have shown a high transparency (more than 75%) in the spectral range from 400 nm to 2000 nm. The optical band gap energy values of the ZnO thin films elaborated are located around 3.22 eV. Room temperature photoluminescence is dominated by a strong luminescence peak around 378 nm and a low-intensity peak around 477 nm.

Keywords: Ammonium hydroxide; Sol-gel Method; Photoluminescence; Optical band gap; Process concentration and temperature

Introduction

The transparent conductive oxides (TCO) have attracted much attention for optoelectronic applications such as solar cells and light emitting diodes thanks to their interesting properties. In particular, in thin solar cells, in order to collect the maximum of carriers, a conductive layer covering the totality of the cell surface is essential. A trade-off between the conductor and the transparency of this layer must be obtained which is fulfilled by the TCO layers. The main used TCO as transparent electrodes for solar cells were for a long time the SnO_2 and the ITO. Since the 1980s, a new TCO has been studied; it is the zinc oxide (ZnO) [1]. The ZnO is a II-VI wide bandgap semiconductor material with a direct band gap around 3.2-3.37eV at room temperature making it transparent for the visible light. The photovoltaic devices based on zinc oxide (ZnO) thin films are more stable when exposed to hydrogen plasma unlike to the SnO_2 and ITO whose the optical transmission is deteriorated under this condition [2,3]. Moreover, ZnO is abundant and not toxic in contrary, for example, to the indium in the ITO. Stoichiometric zinc oxide crystallizes with the quartzite structure to form transparent needle-shaped Crystals. The structure contains large voids which can easily accommodate interstitial atoms making the ZnO a natively n-type semi-conductor justified by the presence of excess Zn atoms in the interstitial sites or oxygen vacancies. ZnO can be grown on different substrates and in many forms, such as bulk single crystal, powder, thin film, nanowires, and nanotubes. Furthermore, the electrical properties of ZnO can be easily controlled by altering the concentration of oxygen vacancies or by doping. In addition to that, ZnO thin films have drowned much interest thanks to its ultraviolet emission. It is commonly known that its room temperature photoluminescence spectra usually show three major peaks: a UV peak around 380 nm, a green emission peak around 520 nm, and an emission around 600 nm. The UV peak is justified by an exciton transition as reported by many authors [4,5], while the two broad visible bands are generally attributed to deep-level defects in ZnO crystal, such as vacancies and interstitials of zinc and oxygen [4,6].

ZnO thin films can be prepared by various techniques: Sputtering [7], Chemical Vapor Deposition (CVD) [8], Laser ablation [9], Sol-gel [10,11], Spray pyrolysis [12]. It has been reported that electronic transport, structural and optical properties of ZnO films, especially the photoluminescence, are very sensitive to the preparation method and deposition conditions [13-15].

In the present work, ZnO thin films were prepared by a sol-gel spin coating method and deposited on glass substrates. The Sol-gel process is chosen because it is simple and very cheap route to obtain transparent Zinc oxide films were used based on ammonium hydroxide as an additive thanks to its efficiency to obtain a transparent and homogeneous solution during a short time. The elaborated films were characterized by measuring optical, microstructural and photoluminescence (PL) characteristics. The effect of the precursor concentration and the annealing temperature on ZnO properties is investigated.

Experimental Details

Experimental procedure

Zinc acetate dihydrate ($Zn(CH_3COO)2.2H_2O$) with a different molarity (0.1 M and 0.2 M) and ethanol were used as starting materials. The solution with pH=10 was prepared by dissolving 0.10975 g of zinc acetate dihydrate in 4 mL of ethanol. In order to obtain a clear and homogeneous solution, 1 mL of ammonium hydroxide (NH_4OH) was added and final step, the solution was filtered. The mixture was stirred by a magnetic stirrer at room temperature for 30 min and then was aged for 24 hours. The ZnO thin films were deposited by a spin-coating method on cleaned and dried glass substrates. The solution was spin-

***Corresponding author:** Wannes HB, Photovoltaic Laboratory, Center for Research and Energy Technologies, Borj-Cedria Technopole, Tunisia, Tel: (+216) 79 325 160; E-mail: benwannes.haifa00@gmail.com

Received December 08, 2017; **Accepted** December 22, 2017; **Published** January 20, 2018

Citation: Wannes BH, Zaghouania BR, Dimassia W (2018) Effect of Experimental Condition on Properties of Zinc Oxide Films Prepared by Sol-Gel Deposition with Ammonium Hydroxide as an Additive. J Textile Sci Eng 8: 329. doi: 10.4172/2165-8064.1000329

coated on the substrates with the speed to 1000 rpm for the 30s. The samples were then heated 100°C for 10 minutes. This process of coating and heating was repeated 12 times [16]. Finally, ZnO thin films were annealed in a muffle furnace at two different temperatures at 400°C and 500°C for two hours under air. The entire process for preparing ZnO films is recapitulated in Figure 1.

Characterization techniques

The coated films have been characterized by different techniques. Microstructural properties were obtained at room temperature using X-ray diffraction (XRD) "PANalytical X'pert Pro MPD" diffractometer equipped with a copper Kα (λ=0.154 nm) radiation source. Optical studies were performed by measuring the transmittance and the reflectance for wavelengths in the range of 200-2000 nm at room temperature using a Shimadzu UV-Vis 900 spectrophotometer. Photoluminescence measurements were carried out at ambient temperature with a 300 nm laser.

Results and Discussions

Structural properties

The X-ray diffraction patterns of the ZnO thin films prepared by spin-coating with different Zinc acetate concentrations (0.1 M and 0.2 M) and different annealing temperature (400°C and 500°C) are presented in Figure 2. It is observed that elaborated ZnO thin films are polycrystalline with hexagonal wurtzite phase. The main X-ray diffraction peaks corresponding to (100), (002) and (101) planes were observed in all the ZnO films. In this case the two preferential orientations: a-axis (100) and c-axis (002) are present; this difference in orientation is attributable to chemical system utilized (the precursor concentration, the nature and the concentration of the additive) i.e., nature of the reactants as well as amorphous substrates such as glass and annealing temperature [17]. Znaidi et al. proposed that the different orientations observed, based on the particle-substrate versus particle–particle interactions [18]. The XRD patterns of the samples indicated enhanced intensities of (002) diffraction peak indicating preferential orientation along the c-axis for sample 0.1 M at 400°C and (100) for other samples.

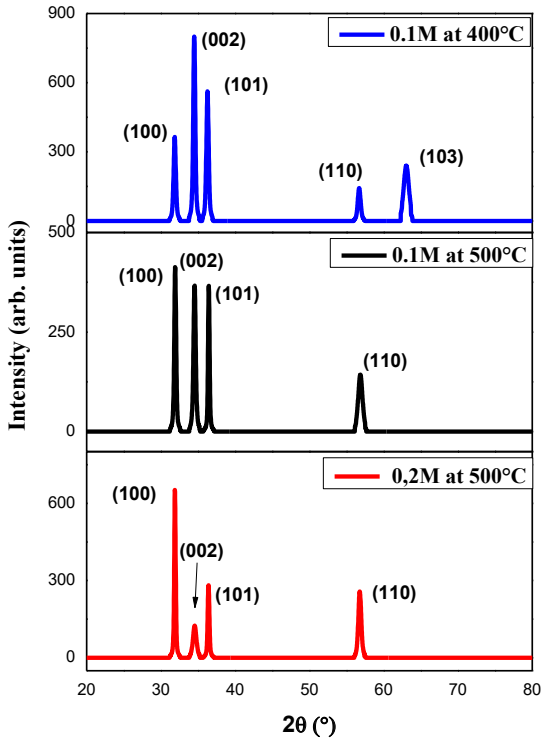

Figure 2: X-Ray diffraction spectra of ZnO films prepared by a 12-cycle spin-coating.

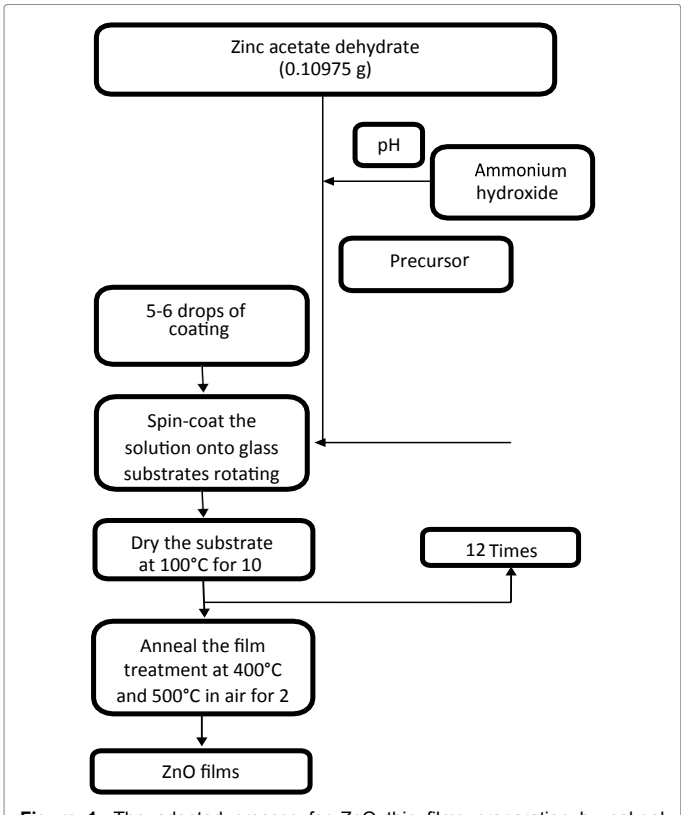

Figure 1: The adopted process for ZnO thin films preparation by sol-gel method.

The interplanar spacing d_{hkl} value of ZnO thin films was also calculated using Bragg equation [19]:

$$2d_{hkl}\sin\theta = n\lambda \quad (1)$$

Both lattice parameters 'a' and 'c' for the hexagonal compact phase are calculated via the (002) and (001) orientations using the following relation [20,21]:

$$\frac{1}{d_{hkl}^2} = \frac{4}{3\alpha^2}\left(h^2 + k^2 + hk\right) + \frac{l^2}{c^2} \quad (2)$$

Table 1 summarizes the calculated parameters of the zinc oxide thin films. The 'a' and 'c' values were in concordance with the standard values of ZnO single crystal indicating the good crystallite of ZnO films was good crystalline in nature [22]. Moreover, it can be seen that the interplanar spacing d_{hkl} decreases with the concentration and temperature increase showing that both of the concentration and temperature play an important role in improving the transparency of films.

On the other hand, the crystallite size of the ZnO films is estimated from the (002) and (100) diffractions peaks using Scherer's formula [23]:

	d_{002}(Å)	d_{100}(Å)	a (Å)	c (Å)	D(nm)	ξ(10-4)	δ (1015) lines/m²
ZnO 0.2 M at T=500°C	2.5951	2.8051	3.239	5.1903	30.82	4.37	1.05
ZnO 0.1 M at T=500°C	2.5961	2.6994	3.235	5.1921	32.49	3.59	0.95
ZnO 0.1 M at T=400°C	2.6001	2.8085	3.243	5.2003	25.78	4.33	1.5

Table 1: Structural parameters of ZnO thin films elaborated with different concentrations and annealing temperatures.

$$D = \frac{k\lambda}{\beta_{\frac{1}{2}} \cos\theta} \quad (3)$$

Where D is the crystallite size, k=0.90 is the Scherer constant, β1/2 is the full width at half maximum (FWHM) of the peak, θ is the Bragg angle of the peak and λ=1.54 A° is the X-ray wavelength. The crystallite size is increasing from 32.49 to 30.82 nm with the increase in Zn concentration from 0.1 M to 0.2 M. The decrease in size above a certain concentration is probably due to the stronger the Zn-base complex. When varying the annealing temperature from 400 to 500°C, the grain size increases from 25.79 to 32.49 nm. The increase in the crystallite size shows the improvement in the film crystallinity this may be due to the fact that is a consisted of zincite (precipitates), ZnO [24]. The microstrain ξ which is an interesting structural parameter of ZnO thin films is calculated using the following relation [25]:

$$\zeta = \frac{\beta \frac{1}{2}}{4 \tan\theta} \quad (4)$$

Where β1/2 is the FWHM of the (002) and (100) peaks and θ is the Bragg angle. The dislocation density (δ) is calculated using the following relation:

$$\delta = \frac{1}{D^2} \quad (5)$$

δ varied from 0.95 × 1015 to 1.5 × 1015 lines/m² depending on the precursor concentration and temperature. The dislocation density decreases when increasing the annealing temperature due to the effect of the temperature on the crystallization of the ZnO films. Furthermore, δ decreases with the increase in Zn concentration due to its role in grain size.

Optical properties

Study of films transparency: The optical transmittance and reflexion of undoped ZnO thin films in the UV–visible regions are presented in Figure 3. All prepared samples showed a high transmittance exceeding 75% within the visible and infrared region proving a high transparency of these films and their absorption are so weak. ZnO thin films in the visible range are efficient as windows layers for solar cells [26,27]. We notice also the absence of interference fringes in transmission spectra due to the surface roughness caused by the spin-coating process. Jlassi et al. have observed interference fringes in the transmittance spectra of undoped ZnO films elaborated by spray pyrolysis technique due to the multiple reflections at the two-layer edge-characterizing a smooth and uniform surface [28]. Furthermore, the transmission coefficient decreases with the concentration increase due to the increase of the grain boundaries causing light scattering. In Figure 3, we notice a sharp absorption edge between 350 nm and 400 nm indicating large grain texture of the films deposited [29]. Besides, it's a characteristic of a semiconductor with direct forbidden energy band gap Eg.

In addition to that, the total reflectivity of the ZnO films is less than 30%. It decreased from 30% in the UV region to about 7% in the visible. The best optical properties are achieved for the oxide film prepared with a temperature annealing of 400°C and a zinc concentration of 0.1 M. The reflectivity of this sample decreases from 16% in the UV to

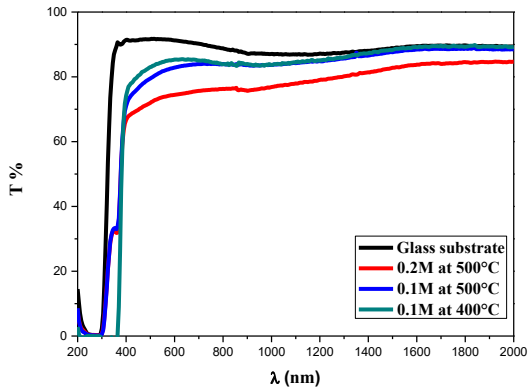

Figure 3: Optical transmittance of ZnO thin films.

7% in the NIR region. This result confirms the transparency and the antireflective behaviour of the ZnO which is beneficial for solar cells. It can also be seen that the interference fringes are absent in reflectance spectra due to weak multiple reflections at the interface as for the transmittance due to the surface roughness. In solar cells, besides to the transparency and the conductivity, the TCO must have another important parameter which is the capacity to diffuse the light. That's why the surface roughness of ZnO is essential as reported by Kluth et al. [30]. The authors have reported on flat ZnO layers deposited by sputtering. They have obtained excellent results thanks to a post-etching process to roughen the ZnO surface [31].

Films thickness: We calculate the film thickness using the method of interference fringes. Using this method, one can determine the film thickness as follows [32]:

$$d = \frac{\lambda_1 \lambda_2}{2(\lambda_1 n_2 - \lambda_2 n_1)} \quad (6)$$

Where: n1 and n2 are the refraction indexes of the film for the wavelengths λ1 and λ2, respectively; we can calculate n1 and n2 from the following relation [32]:

$$n_{1(2)} = \left[N_{1(2)} + \left(N_{1(2)} - s^2 \right)^{\frac{1}{2}} \right]^{\frac{1}{2}} \quad (7)$$

Where: s is the refractive index of the substrate, which is typically 1.52 for the totally transparent glass substrate used in this study and $N_{1(2)}$ can be obtained using this relation [32]:

$$N_{1(2)} = \frac{2s\left(T_M - T_{m1(2)}\right)}{T_M T_{m1(2)}} + \frac{\left(s^2 + 1\right)}{2} \quad (8)$$

Where: $T_{m1(2)}$ is the minimum transmittance corresponds with λ1(λ2) and TM is the maximum transmittance confined between T_{m1} and T_{m2}.

From Table 2 the thickness d decreases when temperatures and concentrations increase, due to the increment of material density owing

ZnO	d(nm)	E_g (eV)	E_u (meV)	E_g/E_u
0.2 M at T=500°C	659.8	3.221	226	14.25
0.1 M at T=500°C	437.79	3.21	220	14.59
0.1 M at T=400°C	308.81	3.197	166	19.26

Table 2: Thickness, Optical band gap energies and Disorder (Urbach energy) Eg and Eu for the different samples.

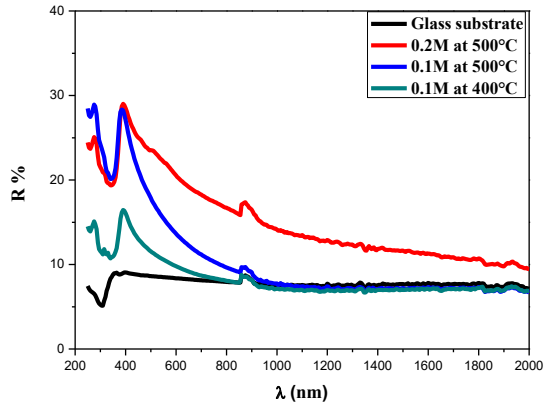

Figure 4: Total reflectivity of ZnO thin films.

to the evaporation of organic residual coming from the precursor solution [33].

The optical band gap: The optical band gap of ZnO thin films was estimated through the determination of the absorption coefficient α calculated from the following expression [34-36]:

$$\alpha = \frac{1}{d}\ln\left(\frac{1}{T}\right) \quad (9)$$

Where T is the transmittance, d is the layer thickness.

In the case of direct transition, the optical band gap Eg is related to the absorption coefficient α via the eqn. (8) [37]:

$$(\alpha h\nu)^2 = \left[A\left(h\nu - E_g\right)\right] \quad (10)$$

Where A is a constant characteristic of the semiconductor and hν is the photon energy.

Figure 5a shows the plot of [αhν] 2 versus the photon energy hν for the different elaborated samples. The intersection of the linear region on the hυ axis gives the Eg, as summarized in Table 2. The optical band gap energy values of the ZnO thin films elaborated are located around 3.22 eV which agrees with the values indicate in literature (3.2-3.3 eV) by many studies [16]. Eg increases partially for increase in microstrain along a-axis or c-axis. The larger optical band-gap was obtained for the ZnO thin film elaborated with 0.1 M at 500°C proving its high crystalline quality [37].

Urbach tailing features: Urbach law of the expression of the absorption coefficient is as follow [38]:

$$\alpha = \alpha_0 \exp\left(\frac{h\nu}{E_u}\right) \quad (11)$$

The width of the located states (band tail energy or Urbach energy Eu) has been estimated from the slopes of (ln α (υ)) versus energy hυ plots of the films:

$$\ln(\alpha) = \ln(\alpha_0) + \frac{h\nu}{E_u} \quad (12)$$

Figure 5b shows the plot of ln(α) versus the photon energy hν for the different elaborated samples. The Urbach energy is a parameter which reflects the power of photonics capture of a semiconductor, thus it changes in accordance with the optical band gap.

Optical and dielectric constants: The refractive index n and extinction coefficient k have been calculated using optical experimental measurements using Bathe and Patil method [39] and Belgacem method [40].

Figure 6 shows the variation of the refractive index n and the extinction index k as a function of the wavelength. The refractive index n presents a maximum at λg (corresponding to Eg value) then it decreases with the wavelength. The evolution of the refractive index is described by the Cauchy model (Figure 7) according to the equation (14) [41]:

$$n(\lambda) = A + \frac{B}{\lambda^2}. \quad (13)$$

Where A and B are the Cauchy's parameters (Table 3) and λ is the wavelength. The extinction coefficient values are lower than 0.1 attributed to the presence of structural defaults on film surface as well as in the bulk such as grain boundaries and dislocations as detailed in XRD analysis described above [42].

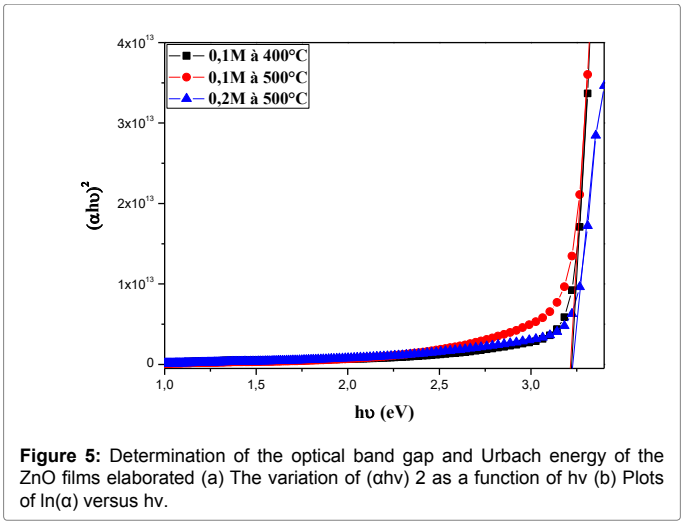

Figure 5: Determination of the optical band gap and Urbach energy of the ZnO films elaborated (a) The variation of (αhν) 2 as a function of hν (b) Plots of ln(α) versus hν.

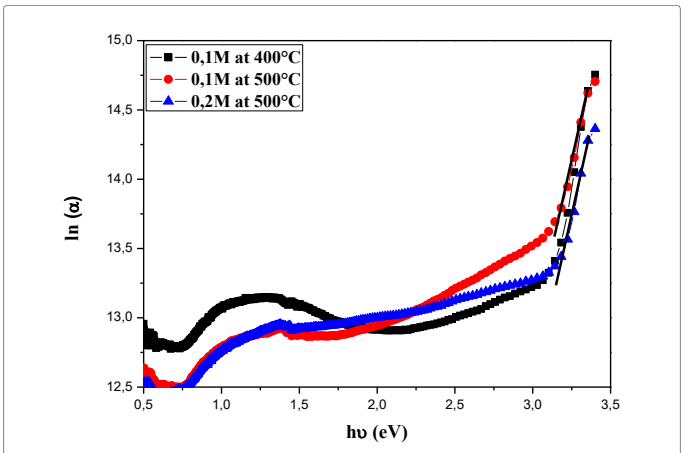

Figure 6: Optical constants as a function of wavelength for the different samples (a) The extinction coefficient (k) (b) The refractive index (n).

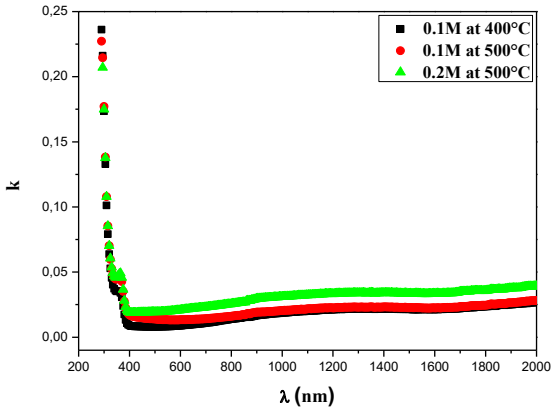

Figure 7: Dispersion of the refractive index (n) by Cauchy fitting for samples elaborated with (a) 0.1M at 400°C (b) 0.1M at 500°C (c) 0.2M at 500°C.

ZnO	A	B(µm-2)
0.2 M at T=500°C	1.88	0.253
0.1 M at T=500°C	1.62	0.21
0.1 M at T=400°C	1.55	0.218

Table 3: Cauchy Model Parameters A and B used for different samples.

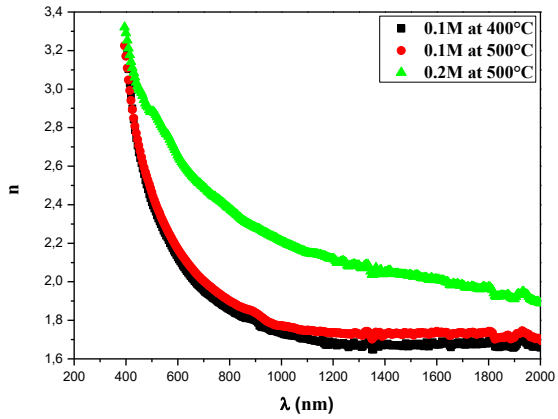

Figure 8: Variation of the dielectric constant of ZnO thin films (a) real part (b) imaginary part.

Figure 8 shows the variation of the dielectric constants ε1 and ε2, as a function of the wavelength. ε1 and ε2 are deduced from n and k according to the following relations [36]:

$$\varepsilon = n^2(\lambda) - K^2(\lambda) \quad (14)$$

$$\varepsilon = 2n(\lambda).k(\lambda) \quad (15)$$

We remark that ε1 has almost the same dependence with wavelength as the refractive index. It is also noticed that the values of the real part are higher than the imaginary part showing the transparency of the films [21].

PL analysis

Figure 9 shows the PL spectra of the different samples. PL spectra of ZnO thin films exhibit two emission bands in UV region corresponding to the band-to-band transition known still by the excitonic emission and a second enough wide corresponding to the emission band visible

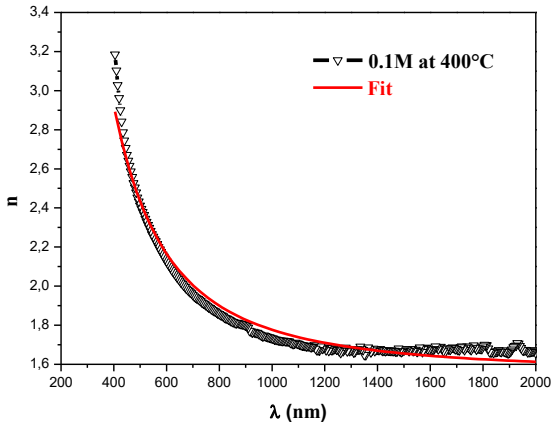

Figure 9: The PL spectra of ZnO thin films of samples prepared (a) for different concentrations (b) for different annealing temperatures.

linked to the deep level defects such as oxygen vacancies or charged zinc vacancies. As observed, the ZnO PL is dominated by a strong luminescence peak at ~378-380 nm for different concentrations and temperatures is due to near band-edge excitonic emission of the wide band gap ZnO. We notice also a low-intensity peak at 477 nm.

The UV emission peak intensity is diminished with the precursor molarity decrease. The shift of band gap energy is related to the structural property. Since ZnO thin film has a tensile built-in strain, the tensile strain in ZnO could be relaxed by providing sufficient thermal energy. If the tensile strain is relaxed, the band gap energy is decreased [42]. Furthermore, as the ZnO films were grown without any intentional doping, the origin of the weak PL emission at ~477 nm may be explained by the transition from the bottom of the conduction band to oxygen-related defects.

We also notice that green-yellow PL intensity increases with increasing annealing temperature from 400 to 500°C. In fact, the annealing in the neutral atmosphere may remove the interstitial oxygen first and then generate singly ionized oxygen vacancy responsible for this emission [6]. Moreover, the broad green-yellow luminescence of ZnO thin films is related to the amount of non-stoichiometric intrinsic defects [43,44]. On the other hand, the observed red shift in UV emission peak and the little variation for the other emissions certainly due to the fact that, since there is increasing film thickness [11].

Conclusion

The effect of experimental condition on physical properties of high transparent ZnO thin films using ammonium hydroxide as an additive by the low-cost sol-gel method with different precursor concentrations and annealing temperatures has been investigated. XRD study shows that all ZnO thin films prepared are in polycrystalline hexagonal wurtzite state with preferred growth orientations along the a-axis (100) and c-axis (002) planes. The grain size of crystallites decreases with the increase of Zn concentrations and with temperature decrease from 26 nm for 0.1 M at 400°C to 30 nm for 0.2 M at 500°C. All ZnO films are highly transparent with a transmittance more than 75%. The high quality of the films is confirmed by the low value of the extinction coefficient which was calculated from optical absorption curves. Finally, room temperature photoluminescence reveals that the UV peak positions are dominated by a strong luminescence peak (excitonic emission) at around 378 nm indicative a reasonably good crystalline quality.

References

1. Ginley SD, Bright C (2000) Transparent conducting oxides, MRS Bulletin. 25: 15.
2. Caillaud F, Smith A, Baumard FJ (1992) Additives content in ZnO films prepared by spray pyrolysis. J Eur Ceram Soc 9: 447.
3. Seeber TW, Abou-Helal OM, Bath S, Beil D, Höche T, et al. (1999) Transparent semiconducting ZnO: Al thin films prepared by spray pyrolysis, Mater Sci Semicond Process 2: 45.
4. Lin B, Fu Z (2001) Green luminescent center in undoped zinc oxide films deposited on silicon substrates, Appl Phys Lett 79: 943.
5. Chu S, Olmedo M, Yang Z, Kong J, Liu J (2008) Electrically pumped ultraviolet ZnO diode lasers on Si. Appl Phy Lett 93: 181106.
6. Vanheusden K, Seager HC, Warren LW, Tallant RD, Caruso J, et al. (1997) Green photoluminescence efficiency and free-carrier density in ZnO phosphor powders prepared by spray pyrolysis. J Lumin 75: 11.
7. Moustaghfir A, Tomasella E, Ben Amor S, Jcquet M, Cellier J, et al. (2003) Structural and optical studies of ZnO thin films deposited by r.f magnetron sputtering: influence of annealing. Surf Coat Technol 174: 175-193.
8. Haga K, Kamidaira M, Kashiwaba Y, Sekiguchi T, Watanabe H (2000) ZnO thin films prepared by remote plasma-enhanced CVD method. J Cryst Growth 77: 214-215.
9. Narasimhan LK, Pai PS, Palkar RV, Pinto R (1997) High quality zinc oxide films by pulsed laser ablation, Thin Solid Films 295: 104.
10. Wannes BH, Zaghouani RB, Ouertani R, Araújo A, Mendes JM, et al. (2018) Study of the stabilizer influence on the structural and optical properties of sol-gel spin coated zinc oxide films. Mat Sci in Semi Processing 74: 80-87.
11. Znaidi L, Chauveau T, Tallaire A, Liu F, Rahmani M, et al. (2015) Textured ZnO thin films by sol-gel process: Synthesis and characterizations. Thin Solid Films 617: 156.
12. Paraguay FD, Estrada L, Acosta N, Andrade E, Miki-Yoshida M (1999) Growth structure and optical characterization of high quality ZnO thin films obtained by spray pyrolysis. Thin Solid Films 350: 192.
13. Chopra LK, Major S, Pandya KD (1983) Transparent conductors - A status review. Thin Solid Films 102: 1-46.
14. Van de Pol MCF, Blom RF, Popma RF (1991) planar magnetron sputtered ZnO films: Structural properties. University of Twente 204: 349-364.
15. Sang B, Yamada A, Konagai M (1998) Highly Stable ZnO Thin Films by Atomic Layer Deposition. Japanese Journal of Applied Physics, 37: 10A.
16. Smirnov M, Baban C, Rusu IG (2010) Structural and optical characteristics of spin-coated ZnO thin films, Appl Surf Sci 256: 2405.
17. Chittofrati A, Matijević E (1990) Uniform particles of zinc oxide of different morphologies, Colloids Surf. Elsevier Science Publishers 48: 65-78.
18. Znaidi L, Soler Illia AAJG, Benyahia S, Sanchez C, Kanaev VA (2003) Oriented ZnO thin films synthesis by sol–gel process for laser application. Thin Solid Films 428: 257-262.
19. Lupan O, Pauporte T, Chow L, Viana B, Pelle F, et al. (2010) Effects of annealing on properties of ZnO thin films prepared by electrochemical deposition in chloride medium. Appl Surf Sci 256: 1895.
20. Peng PL, Fang L, Yang FX, Li JY, Huang LQ, et al. (2009) Effect of annealing temperature on the structure and optical properties of In-doped ZnO thin films. J Alloys Compd 484: 575.
21. Boukhachem A, Ouni B, Karyaoui M, Madani A, Chtourou R, et al. (2012) Structural, opto-thermal and electrical properties of ZnO:Mo sprayed thin films, Mater. Sci. Semicond. Process 15: 282-292.
22. Amutha C, Dhanalakshmi A, Lawrence B, Kulathuraan K, Ramadas V, et al. (2014) Influence of Concentration on Structural and Optical Characteristics of Nanocrystalline ZnO Thin Films Synthesized by Sol- Gel Dip Coating Method. Progr Nanotechnol Nanomater 3: 13-18.
23. Benramache S, Rahal A, Benhaoua B (2014) The effects of solvent nature on spray-deposited ZnO thin film prepared from Zn (CH3COO)2, 2H2O. Optik 125: 663-666.
24. Chittofrati A, Matijevi E (1990) Colloids Surf. 48: 65-78.
25. Sahay PP, Nath KR (2008) Al-doped ZnO thin films as methanol sensors, Sens. Actuators. Bio Chem 134: 654.
26. Chopra LK, Das SR (1983) Thin Film Solar Cells, first ed., Springer, New York, 1983.
27. Kazmerski LL (1980) Polycrystalline and Amorphous Thin Films and Devices. Academic Press, New York 28 August, 1980.
28. Jlassi M, Sta I, Hajji M, Ezzaouia H (2014) Effect of nickel doping on physical properties of zinc oxide thin films prepared by the spray pyrolysis method. Appl Surf Sci 301: 216.
29. Gayen RN, Sarkar K, Hussain S, Bhar R, Pal KA (2011) ZnO films prepared by modified sol-gel technique, INDIAN J PURE & APPL PHYS. 49: 470-477.
30. Kluth O, Löffl A, Wieder S, Beneking C, Appenzeller W, et al. (1997) ISI-PV, D-52425 Jülich, Germany, Texture etched Al-Doped ZnO: A new material for enhanced light trapping in thin film solar cells.
31. Rech B, Wieder S, Beneking C, Löffl A, Wagner H, et al. (1997) Texture etched ZnO:Al films as front contact and back reflector in amorphous silicon P-I-N and N-I-P solar cells. IEEE.
32. Swanepoel R (1983) Determination of the thickness and optical constants of amorphous silicon, J Phps E: Sci Instrum Vol: 16.:1214.
33. Dahnoun M, Attaf A, Saidi H, Yahia A, Khelifi C (2017) Structural, optical and electrical properties of zinc oxide thin films deposited by sol-gel spin coating technique. Optik-International Journal for Light and Electron Optics 134: 53-59.
34. Rusu IG, Popa Em, Rusu GG, Salaoru I (2003) On the electronic transport properties of polycrystalline ZnSe films. Appl Surf Sci 218: 222-230.
35. Pankove IJ (1971) Optical Processes in Semiconductors, Dover, New York.
36. Chopra LK (1969) Thin Film Phenomena, McGraw-Hill, New York.
37. Shinde RV, Gujar PT, Lokhande CD (2007) LPG sensing properties of ZnO films prepared by spray pyrolysis method: Effect of molarity of precursor solution, Sens. Actuators. B: Chem. 120: 551.
38. Urbach F (1953) The long-wavelength edge of the photographic sensitivity and of the electronic absorption of solids. Physical Review 92: 1324.
39. Bathe RS, Patil SP (2007) Electrochromic characteristics of fibrous reticulated WO 3 thin films prepared by pulsed spray pyrolysis technique . Sol Energy Mater Sol Cells 91: 1097-1101.
40. Belgacem S, Bennaceur R (1990) Propriétés optiques des couches minces de SnO2 et CuInS2 airless spray. Rev Phys Appl 25: 1245.
41. Tompkins GH, McGahan WA (1999) Spectroscopic Ellipsometry and Reflectometry: A User's Guide, John Wiley & Sons Inc, New York, 1999.
42. Boughalmi R, Boukhachem A, Kahlaoui M, Maghraoui H, Amlouk M (2014) Physical investigations on Sb2S3 sprayed thin film for optoelectronic applications, Mater. Sci Semicond Process 26: 593.
43. Kang SH, Kang SJ, Kim WJ, Lee YS (2004) Annealing effect on the property of ultraviolet and green emissions of ZnO thin films. J Appl Phys 95: 1246.
44. Kim SY, Tai PW, Shu JS (2005) Effect of preheating temperature on structural and optical properties of ZnO thin films by sol–gel process. Thin Solid Films 491: 153.